Modeling hurricane impacts on beaches, dunes and barrier islands

Dano Roelvink[1,2,3], Ad Reniers[3,4], Ap van Dongeren[2], Jaap van Thiel de Vries[2,3], Jamie Lescinski[2], Dirk-Jan Walstra[2,3]

[1)]UNESCO-IHE Institute for Water Education, p.o. box 3015, 2601 DA Delft, the Netherlands, d.roelvink@unesco-ihe.org, +31 15 2151838
[2)]WL | Delft Hydraulics
[3)]Delft University of Technology
[4)]Rosenstiel School of Marine and Atmospheric Science, Univ. of Miami

1 INTRODUCTION

The devastating effects of hurricanes on low-lying sandy coasts, especially during the 2004 and 2005 seasons have pointed at an urgent need to be able to assess the vulnerability of coastal areas and (re-)design coastal protection for future events, but also to evaluate the performance of existing coastal protection projects compared to 'do-nothing' scenarios.

In order to address such questions the Morphos-3D project was initiated. This project brings together models, modelers and data on hurricane winds, storm surges, wave generation and nearshore processes (wave breaking, surf and swash zone processes, dune erosion, overwashing and breaching). For modeling nearshore processes the authors were funded by the European Research Office of USACE-ERDC to provide advice and algorithms, After some iterations the best way to do this was found to be the development of an open-source program dedicated to this problem. This program was given the name of XBeach for eXtreme Beach behavior model,

2 PROCESSES

Sallenger (2000) defines an Impact Level to denote different regimes of impact on barrier islands by hurricanes: these levels are 1) swash regime, 2) collision regime, 3) overwash regime and 4) inundation regime. Our aim is to model all these regimes seamlessly and in a horizontally 2D setting. The following processes have to be considered when modeling these responses.

- **Dune erosion.** The development of a scarp, and episodic slumping after undercutting is a dominant process. This supplies sand to the swash and surf zone that is transported seaward by the backwash motion and by the undertow. Models such as DUROSTA (Steetzel, 1993) focus on the offshore transport and obtain the supply of sand by extrapolating these transports to the dry dune. Overton and Fisher (1988), Nishi and Kraus (1996) focus on the supply of sand by the dune based on the concept of Wave Impact. Both approaches rely on heuristic estimates of the runup and are well suited for 1D application but difficult to apply in a horizontally 2D setting.
- **Swash, surf beat.** Raubenheimer and Guza (1996) show that incident band swash is saturated, infragravity swash is not, therefore infragravity swash is dominant in storm conditions. Models range from empirical formulations (e.g. Stockdon et al, 2006)

through analytical approaches (Schaeffer, 1994, Erikson et al, 2005) to numerical models in 1D (e.g. Roelvink, 1993b) and 2DH (e.g. van Dongeren et al, 2003, Reniers et al, 2004). Short wave averaged models are very well capable of describing low-frequency motions. For such a model to be applied for swash, a robust drying/flooding formulation is needed, guaranteeing momentum conservation, e.g. Stelling and Duinmeijer (2006).

- **Forcing by short waves.** This can be derived from the time-varying wave action balance e.g. Phillips (1977) with dissipation by breaking. Roelvink (1993) formulated a dissipation model for use in combination with wave group variation. A roller model (Svendsen, 1984, Nairn et al, 1990, Stive and de Vriend. 1994) is needed to represent momentum stored in surface rollers which leads to a shoreward shift in forcing. In Reniers et al (2004) the time-varying wave energy balance is solved over a single direction given by SWAN.
- **Overwashing.** This process is dominated by low-frequency motions on the time-scale of wave groups. It is an important landward transport process. Some heuristic approaches exist in 1D, e.g. in the SBeach overwash module (Larson et al, 2004). Even more than for swash impacting the dune front, these motions are dominated by low-frequency waves.
- **Breaching.** Visser (1998) presents a semi-empirical approach, only for schematic uniform cross-section. Roelvink et al 2003 show acceptable performance for breaching of sand barrier using combination of shallow water equations and standard suspended transport model, plus simple bank erosion mechanism to represent breach widening.
- **Return flow.** This keeps the erosion process going by removing sand from the slumping dune face. Various models have been proposed for vertical profile of current, see Reniers et al. (2004b) for a review. The vertical variation is not very strong during extreme conditions and sometimes neglected; the roller contribution to the undertow may be strong.
- **Longshore current.** This may have a large impact on cross-shore transport because of increased concentrations; usually this is not taken into account. It depends on forcing and bed shear stress. There are many wave-current interaction models for waves plus current at fixed bottom (e.g. Soulsby, 1993); often no effect of sand bed forms is taken into account. This complicates the modeling considerably; Ruessink et al (2001) show good skill while assuming simple constant c_f value.
- **Suspended and bedload transport.** The surf and swash zone sediment transport processes are very complex, with sediment stirring by a combination of short-wave and long-wave orbital motion, current and breaker-induced turbulence. We expect suspended transport by far to dominate during extreme conditions, and believe intra-wave processes due to wave asymmetry and wave skewness to be relatively minor compared to long-wave and mean currents. Reniers et al. (2004a) successfully applied a relatively simple and transparent formulation according to Soulsby – Van Rijn (Soulsby, 1997) in a short-wave averaged but long wave resolving model of surf zone processes; Roelvink et al. (2003) used similar formulations to model barrier breaching.

3 OBJECTIVE

The main objective of the XBeach model is to provide a robust and flexible environment in which to test morphological modeling concepts for the case of dune erosion, overwashing and

breaching. The top priority is to provide numerical stability; first order accuracy is accepted since there is a need for small space steps and time steps anyway, to represent the strong gradients in space and time in the nearshore and swash zone. Because of the many shock-like features in both hydrodynamics and morphodynamics we choose upwind schematizations as a means to avoid numerical oscillations which can be deadly in shallow areas.

The modeling environment should be flexible and the code easy to comprehend and concise; besides, performance and portability are important issues. Therefore we have adopted Fortran 90/95 as the programming language.

4 CONTEXT

The XBeach model can be used as stand-alone model for small-scale (project-scale) coastal applications, but will also be used within the Morphos model system, where it will be driven by boundary conditions provided by the wind, wave and surge models and its main output to be transferred back will be the time-varying bathymetry and possibly discharges over breached barrier island sections. The model solves coupled 2D horizontal equations for wave propagation, flow, sediment transport and bottom changes, for varying (spectral) wave and flow boundary conditions. Because the model takes into account the variation in wave height in time (long known to surfers) it resolves the special long wave motions created by this variation. This so-called ‘surf beat’ is responsible for most of the swash waves that actually hit the dune front or overtop it. Because of this innovation the XBeach model is better able to model the development of the dune erosion profile, to predict when a dune or barrier island will start overwashing and breaching and to model the developments throughout these phases.

5 MODEL FORMULATIONS

Coordinate system and grid

XBeach uses a coordinate system where the computational x-axis is always oriented towards the coast, approximately perpendicular to the coastline, and the y-axis is alongshore. This coordinate system is defined relative to world coordinates (xw,yw) through the origin (xori,yori) and the orientation alfa, defined counter-clockwise w.r.t. the xw-axis (East).

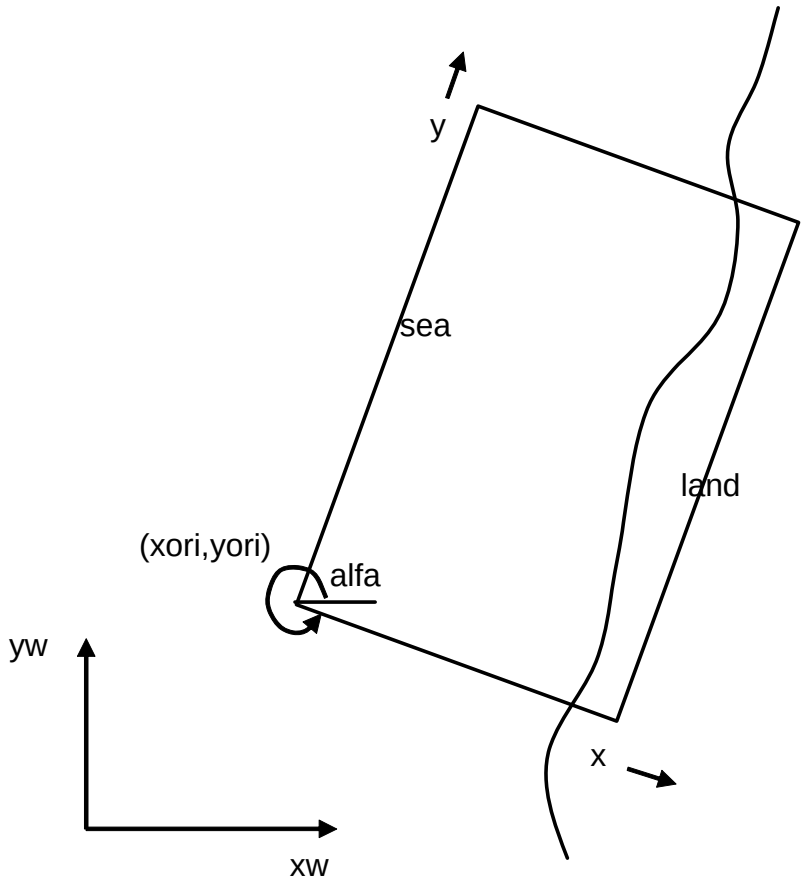

Figure 1 Coordinate system

The grid applied is a rectilinear, non-equidistant, staggered grid, where the bed levels, water levels, water depths and concentrations are defined in cell centers, and velocities and sediment transports are defined in u- and v-points, viz. at the cell interfaces. In the wave energy balance, the energy, roller energy and radiation stress are defined at the cell centers, whereas the radiation stress gradients are defined at u- and v-points.

Wave action equation

The wave forcing in the shallow water momentum equation is obtained from a time dependent version of the wave action balance equation. Similar to Delft University's HISWA model, the directional distribution of the action density is taken into account whereas the frequency spectrum is represented by a single mean frequency. The wave action balance is then given by:

$$\frac{\partial A}{\partial t}+\frac{\partial c_x A}{\partial x}+\frac{\partial c_y A}{\partial y}+\frac{\partial c_\theta A}{\partial \theta}=-\frac{D}{\sigma} \qquad (5.1)$$

with the wave action:

$$A(x,y,\theta)=\frac{S_w(x,y,\theta)}{\sigma(x,y)} \qquad (5.2)$$

where S_w represents the wave energy in each directional bin and σ the intrinsic wave frequency. The wave action propagation speeds in x- and y-direction are given by:

$$c_x(x,y,\theta) = c_g(x,y)\bullet\cos(\theta) + u(x,y)$$
$$c_y(x,y,\theta) = c_g(x,y)\bullet\sin(\theta) + v(x,y) \tag{5.3}$$

where θ represents the angle of incidence with respect to the x-axis. The propagation speed in θ-space is obtained from:

$$c_\theta(x,y,\theta) = \frac{\sigma}{\sinh 2kh}\left(\frac{\partial h}{\partial x}\sin\theta - \frac{\partial h}{\partial y}\cos\theta\right) + \cos\theta\left(\sin\theta\frac{\partial u}{\partial x} - \cos\theta\frac{\partial u}{\partial y}\right) + \\ + \sin\theta\left(\sin\theta\frac{\partial v}{\partial x} - \cos\theta\frac{\partial v}{\partial y}\right) \tag{5.4}$$

taking into account bottom refraction (first term on the RHS) and current refraction (last two terms on the RHS). The wave number k is obtained from the eikonal equations:

$$\frac{\partial k_x}{\partial t} + \frac{\partial \omega}{\partial x} = 0$$
$$\frac{\partial k_y}{\partial t} + \frac{\partial \omega}{\partial y} = 0 \tag{5.5}$$

where the subscripts refer to the direction of the wave vector components and ω represents the absolute radial frequency. The wave number is then obtained from:

$$k = \sqrt{k_x^2 + k_y^2} \tag{5.6}$$

The absolute radial frequency is given by:

$$\omega = \sigma + \vec{k}\bullet\vec{u} \tag{5.7}$$

and the intrinsic frequency is obtained from the linear dispersion relation:

$$\sigma = \sqrt{gk\tanh kh} \tag{5.8}$$

The group velocity is obtained from linear wave theory:

$$c_g = nc = \left(\frac{1}{2} + \frac{kh}{\sinh 2kh}\right)\frac{\sigma}{k} \tag{5.9}$$

This concludes the advection of wave action. The wave energy dissipation due to wave breaking is modelled according to Roelvink (1993b);

$$\bar{D} = 2\alpha Q_b f_{m01} E_w$$
$$Q_b = 1\text{-}\exp\left(-(\frac{\mathrm{H}}{\gamma \mathrm{h}})^{\mathrm{n}}\right), \quad H = \sqrt{\frac{8E_w}{\rho g}} \tag{5.10}$$

with $\alpha = O(1)$ and f_{m01} representing the mean intrinsic frequency. (5.11)

Next the total wave dissipation, $\bar{D}$, is distributed proportionally over the wave directions:

$$D(x, y, \theta) = \frac{S_w(x, y, \theta)}{E_w(x, y)} \bar{D} \tag{5.12}$$

This closes the set of equations for the wave action balance. Given the spatial distribution of the wave action and therefore wave energy the wave forcing can be calculated utilizing the radiation stress tensor:

$$\begin{aligned} F_x &= -\left(\frac{\partial S_{xx}}{\partial x} + \frac{\partial S_{xy}}{\partial y} \right) \\ F_y &= -\left(\frac{\partial S_{xy}}{\partial x} + \frac{\partial S_{yy}}{\partial y} \right) \end{aligned} \tag{5.13}$$

And:

$$\begin{aligned} S_{xx} &= \int \left(\frac{c_g}{c} \left(1 + \cos^2 \theta \right) - \frac{1}{2} \right) S_w d\theta \\ S_{xy} &= S_{yx} = \int \sin\theta \cos\theta \left(\frac{c_g}{c} S_w \right) d\theta \\ S_{yy} &= \int \left(\frac{c_g}{c} \left(1 + \sin^2 \theta \right) - \frac{1}{2} \right) S_w d\theta \end{aligned} \tag{5.14}$$

We use an up-wind schematisation to solve the wave action balance.

Roller energy balance

The roller energy balance is coupled to the wave action/energy balance where dissipation of wave energy serves as a source term for the roller energy balance. Similar to the wave action the directional distribution of the roller energy is taken into account whereas the frequency spectrum is represented by a single mean frequency. The roller energy balance is then given by:

$$\frac{\partial S_r}{\partial t} + \frac{\partial c_x S_r}{\partial x} + \frac{\partial c_y S_r}{\partial y} + \frac{\partial c_\theta S_r}{\partial \theta} = -D_r + D_w \tag{5.15}$$

with the roller energy:

$S_r(x, y, \theta)$

representing the roller energy in each directional bin. The roller energy propagation speeds in x- and y-direction are given by:

$$\begin{aligned} c_x(x, y, \theta) &= c(x, y) \bullet \cos(\theta) + u(x, y) \\ c_y(x, y, \theta) &= c(x, y) \bullet \sin(\theta) + v(x, y) \end{aligned} \tag{5.16}$$

where θ represents the angle of incidence with respect to the x-axis. The propagation speed in θ-space is obtained from:

$$c_\theta(x,y,\theta) = \frac{\sigma}{\sinh 2kh}\left(\frac{\partial h}{\partial x}\sin\theta - \frac{\partial h}{\partial y}\cos\theta\right) + \\ + \cos\theta\left(\sin\theta\frac{\partial u}{\partial x} - \cos\theta\frac{\partial u}{\partial y}\right) + \sin\theta\left(\sin\theta\frac{\partial v}{\partial x} - \cos\theta\frac{\partial v}{\partial y}\right) \tag{5.17}$$

taking into account bottom refraction (first term on the RHS) and current refraction (last two terms on the RHS). Hence, we are assuming that the waves and rollers propagate in the same direction. The phase velocity is obtained from linear wave theory:

$$c = \frac{\sigma}{k} \tag{5.18}$$

which concludes the advection of roller energy. The roller energy dissipation is given by (Deigaard, 1993):

$$\bar{D}_r = c\tau_r \tag{5.19}$$

with τ_r representing the shear stress induced by the roller at the surface, which is expressed by (Svendsen, 1984):

$$\tau_r = \frac{\rho g R}{L}\beta_r \tag{5.20}$$

where *R* represents the roller area and β_r is the slope of the breaking wave. The roller area is related to the roller energy trough:

$$E_r = \frac{1}{2}\frac{\rho R c^2}{L} \tag{5.21}$$

Next the total wave dissipation, $\bar{D}_r$, is distributed proportionally over the wave directions:

$$D_r(x,y,\theta) = \frac{S_r(x,y,\theta)}{E_r(x,y)}\bar{D}_r \tag{5.22}$$

Similarly, the source term is obtained from the wave action/energy balance:

$$D_w(x,y,\theta) = \frac{S_w(x,y,\theta)}{E_w(x,y)}\bar{D} \tag{5.23}$$

This closes the set of equations for the roller energy balance. The roller also affects the wave forcing and has therefore to be included in the radiation stress terms:

$$S_{xx,r} = \int \cos^2\theta S_r d\theta$$
$$S_{xy,r} = S_{yx,r} = \int \sin\theta\cos\theta S_r d\theta \qquad (5.24)$$
$$S_{yy,r} = \int \sin^2\theta S_w d\theta$$

These roller radiation stress contributions are added to the wave-induced radiation stresses. Similar to the solution of the wave action equations we use an up-wind schematisation to solve the roller energy balance.

Shallow water equations

For the low-frequency and mean flows we use the shallow water equations, in first instance neglecting Coriolis and horizontal diffusion terms:

$$\frac{\partial u}{\partial t} + u\frac{\partial u}{\partial x} + v\frac{\partial u}{\partial y} = \frac{\tau_{sx}}{\rho h} - \frac{\tau_{bx}}{\rho h} - g\frac{\partial \eta}{\partial x} + \frac{F_x}{\rho h} \qquad (5.25)$$

$$\frac{\partial v}{\partial t} + u\frac{\partial v}{\partial x} + v\frac{\partial v}{\partial y} = +\frac{\tau_{sy}}{\rho h} - \frac{\tau_{by}}{\rho h} - g\frac{\partial \eta}{\partial y} + \frac{F_y}{\rho h} \qquad (5.26)$$

$$\frac{\partial \eta}{\partial t} + \frac{\partial hu}{\partial x} + \frac{\partial hv}{\partial y} = 0 \qquad (5.27)$$

Here, h is the water depth, u, v are velocities in x and and y direction, τ_{bx}, τ_{by} are the bed shear stresses, g is the acceleration of gravity, η is the water level and F_x, F_y are the wave-induced stresses.

We apply a staggered grid, where bed levels and water levels are defined in the centre of cells, and velocity components at the cell interfaces. An explicit scheme with an automatic time step is applied; the discretization is similar to Stelling and Duinmeijer (2006), in the momentum-conserving form, which is especially suitable for drying and flooding and which allows a combination of sub- and supercritical flows.

Generalized Lagrangian Mean (GLM) formulations.

To account for the wave induced mass-flux and the subsequent (return) flow the shallow water equations are cast into a Generalized Lagrangian Mean (GLM) formulation (Walstra et al, 2000). To that end the Eulerian shallow water velocity u^E is replaced with its lagrangian equivalent, u^L:

$$u^L = u^E + u^S \quad and \quad v^L = v^E + v^S \qquad (5.28)$$

and u^S , v^S represents the Stokes drift in x- and y-direction respectively (Phillips, 1977):

$$u^S = \frac{E_w \cos\theta}{\rho hc} \quad and \quad v^S = \frac{E_w \sin\theta}{\rho hc} \qquad (5.29)$$

where the wave-group varying short wave energy and direction are obtained from the wave-action balance. The resulting GLM-momentum equations are given by:

$$\frac{\partial u^L}{\partial t} + u^L \frac{\partial u^L}{\partial x} + v^L \frac{\partial u^L}{\partial y} = -\frac{\tau_{bx}^E}{\rho h} - g\frac{\partial \eta}{\partial x} + \frac{F_x}{\rho h}$$
$$\frac{\partial v^L}{\partial t} + u^L \frac{\partial v^L}{\partial x} + v^L \frac{\partial v^L}{\partial y} = -\frac{\tau_{by}^E}{\rho h} - g\frac{\partial \eta}{\partial y} + \frac{F_y}{\rho h} \qquad (5.30)$$

for the x- and y-direction respectively. This operation shows that the GLM equations for the depth-averaged flow are very similar to the previously described Eulerian formulation, with the exception of the bottom shear stress terms that are calculated with the Eulerian velocities as experienced by the bed:

$$u^E = u^L - u^S \quad and \quad v^E = v^L - v^S \qquad (5.31)$$

and not with the GLM velocities. Also, the boundary condition for the flow computations has to be expressed in functions of (u^L , v^L) and not (u^E, v^E).

Sediment transport

The sediment transport is modeled with a depth-averaged advection diffusion equation [Galappatti, 1983]:

$$\frac{\partial hC}{\partial t} + \frac{\partial hCu^E}{\partial x} + \frac{\partial hCv^E}{\partial y} + \frac{\partial}{\partial x}\left[D_h h \frac{\partial C}{\partial x} \right] + \frac{\partial}{\partial y}\left[D_h h \frac{\partial C}{\partial y} \right] = \frac{hC_{eq} - hC}{T_s} \qquad (5.32)$$

where C represents the depth-averaged sediment concentration which varies on the infragravity time scale. The entrainment of the sediment is represented by an adaptation time T_s, given by a simple approximation based on the local water depth, h, and sediment fall velocity w_s:

$$T_s = \max\left(0.05\frac{h}{w_s}, 0.2 \right) s \qquad (5.33)$$

where a small value of T corresponds to nearly instantaneous sediment response. The entrainment or deposition of sediment is determined by the mismatch between the actual sediment concentration and the equilibrium concentration, C_{eq}, thus representing the source term in the sediment transport equation.

The bed-update is discussed next. Based on the gradients in the sediment transport the bed level changes according to:

$$(1-p)\frac{\partial z_b}{\partial t} + \frac{\partial S_x}{\partial x} + \frac{\partial S_y}{\partial y} = 0 \qquad (5.34)$$

where *p is the porosity and* S_x and S_y represent the sediment transport rates in *x*- and *y*-direction respectively, given by:

$$S_{x,i,j}^n = \left[\frac{\partial hCu^E}{\partial x} \right]_{i,j}^n + \left[\frac{\partial}{\partial x}\left[D_h h \frac{\partial C}{\partial x} \right] \right]_{i,j}^n \qquad (5.35)$$

and

$$S^n_{y,i,j} = \left[\frac{\partial hCv^E}{\partial y} \right]^n_{i,j} + \left[\frac{\partial}{\partial y} \left[D_h h \frac{\partial C}{\partial y} \right] \right]^n_{i,j} \quad (5.36)$$

Transport formulations

The equilibrium sediment concentration can be calculated with various sediment transport formulae. At the moment the sediment transport formulation of Soulsby-van Rijn (Soulsby, 1997) has been implemented. The C_{eq} is then given by :

$$C_{eq} = \frac{A_{sb} + A_{ss}}{h} \left(\left(|u^E|^2 + 0.018 \frac{u^2_{rms}}{C_d} \right)^{0.5} - u_{cr} \right)^{2.4} (1 - \alpha_b m) \quad (5.37)$$

where sediment is stirred by the Eulerian mean and infragravity velocity in combination with the near bed short wave orbital velocity obtained from the wave-group varying wave energy. The combined mean/infragravity and orbital velocity have to exceed a threshold value, u_{cr}, before sediment is set in motion. The drag coefficient, C_d, is due to flow velocity only (ignoring short wave effects). To account for bed-slope effects on the equilibrium sediment concentration a bed-slope correction factor is introduced, where the bed-slope is denoted by m and α_b represents a calibration factor. The bed load coefficients A_{sb} and the suspended load coefficient A_{ss} are functions of the sediment grain size, relative density of the sediment and the local water depth (see Soulsby [1997] for details).

Avalanching

To account for the slumping of sandy material during storm-induced dune erosion avalanching is introduced to update the bed-evolution. Avalanching is introduced when a critical bed-slope is exceeded:

$$\left| \frac{\partial z_b}{\partial x} \right| > m_{cr} \quad (5.38)$$

Her we consider that inundated areas are much more prone to slumping and therefore we apply separate critical slopes for dry and wet points.

Boundary conditions waves

For the waves the wave energy density at the offshore boundary is prescribed as a function of y, θ and time. This can be generated based on given spectral parameters or using directional spectrum information. At the lateral boundaries, for wave components entering the domain, the alongshore or along-crest gradient is set to zero, effectively eliminating the notorious ‘shadow zones’ found in many wave models.

Boundary conditions flow

At the seaward and landward (in case of a bay) boundary radiating boundary conditions are prescribed, taking into account the incoming bound long waves, following Van Dongeren and Svendsen (1997).

For the lateral boundaries so-called Neumann boundaries are used, where the longshore water level gradient is prescribed, in this case set to zero. This type of boundary conditions has been shown to work quite well with (quasi-)stationary situations, where the coast can be assumed

to be uniform alongshore outside the model domain. So far we have found that also in case of obliquely incident wave groups this kind of boundary conditions appears to give reasonable results, though rigorous testing still has to be done.

6 TEST CASES

A number of test cases have been carried out, both in 1D and in 2DH mode; below some characteristics are given:

Test	**Purpose**	**Type**	**Dimensions**
Carrier and Greenspan	Check numerical scheme	Analytical	1D
Reflecting long wave	Check damping	Analytical	1D
Humptest	Survival test	Analytical	2DH
Edge waves	Check boundaries, development of edge waves and longshore current	Analytical	2DH
Stationary wave propagation	Check shoaling and dissipation, setup	Lab test LIP11D test 2E	1D
Instationary wave propagation	Check mean and LF wave parameters	Lab test LIP11D test 2E	1D
Dune erosion	Check profile evolution	Lab test LIP11D test 2E	1D
Dune erosion	Check effect of wave period on dune erosion	Lab tests Delta Flume 2005	1D
Dune erosion	Simulate long experiment with varying wave conditions	Lab tests large-scale flume Oregon State	1D
Overwash	Simulate dune erosion followed by overwash and inundation	Schematic case	1D
Hurricane impact	Simulate effect of hurricane on different profiles	Field, Asseteague Island	1D
Extreme inundation	Study breaching, warying water level	Schematic	2DH

For lack of space we will describe only a few of these test cases.

LIP11D Delta Flume 1993 - test 2E

This model test, described in Arcilla et al. (1994), concerned extreme conditions with a raised water level at 4.56 m above the flume bottom, Hm0 wave height of 1.4 m and peak period of 5 s. The model was run for 0.8 hours of hydrodynamic time with a morphological factor of 10, effectively representing a morphological simulation time of 8 hours.

A key element in the modelling is the avalanching algorithm; although the surfbeat waves that are explicitly modelled run up and down the upper beach, without a mechanism to transport sand from dry to wet the dune erosion process will not happen. A relatively simple approach, whereby an underwater critical slope of 0.15 and a critical slope above water of 1.0 were applied, proves to be quite successful in representing the retreat of the upper beach and dune face. A grid resolution of 1 m was applied. In Figure 2 the measured and modelled bed evolution is shown, which looks quite promising in the upper region. The behaviour of the bar at approx. 135 m is not represented well; for this, additional processes such as the effect of surface rollers and wave asymmetry/skewness have to be taken into account.

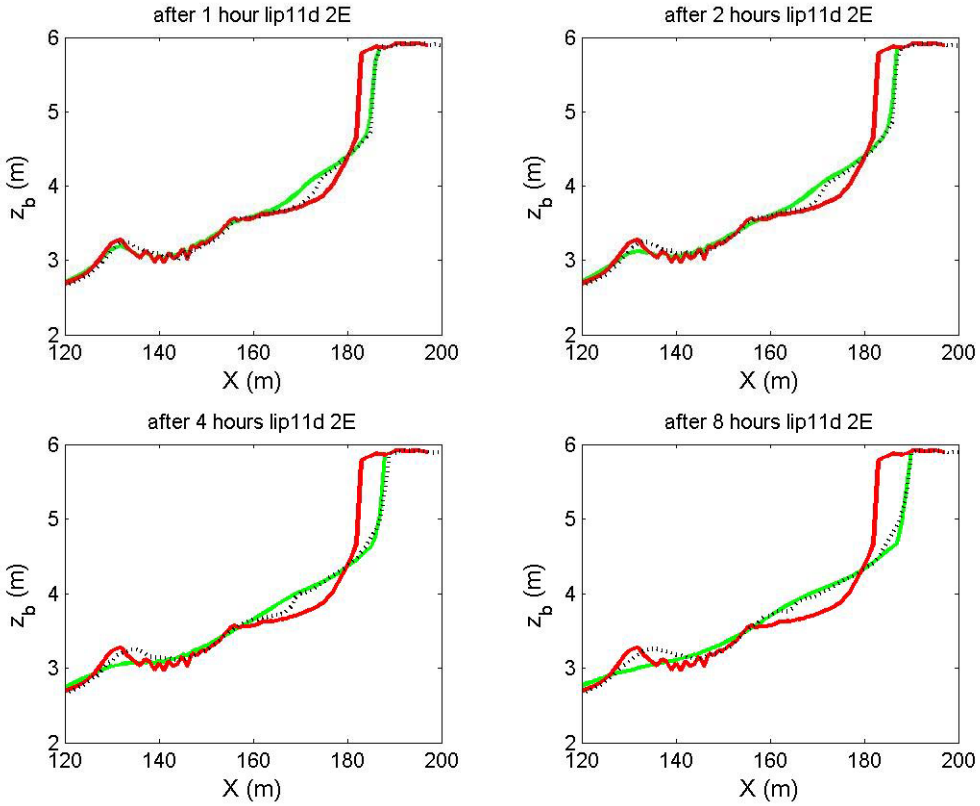

Figure 2. Measured and modelled bed level after 1, 2, 4 and 8 hours of wave action, for a water level of 4.56 m above the flume bottom.

Obliquely incident regular wave groups on planar beach.
This test case was designed to check the seaward and lateral boundary conditions, especially concerning diffraction effects in the generated edge waves and to check the development of the longshore current. The depth runs from 10 m below MSL to + 2.5 m, the incident wave height is 2 m, short wave period 10 s and group period 80 s, with a direction of 30 deg w.r.t. the shore normal.The patterns shown in Figure 3 show that the short wave energy propagates into and out of the model without any noticeable disturbances. The LF water level shown in the second panel from the left shows small regions of somewhat disturbed edge wave patterns at the lateral boundaries, but quite uniform behaviour elsewhere. For the long wave velocity any disturbances are very small, and the longshore current is allowed to develop freely.

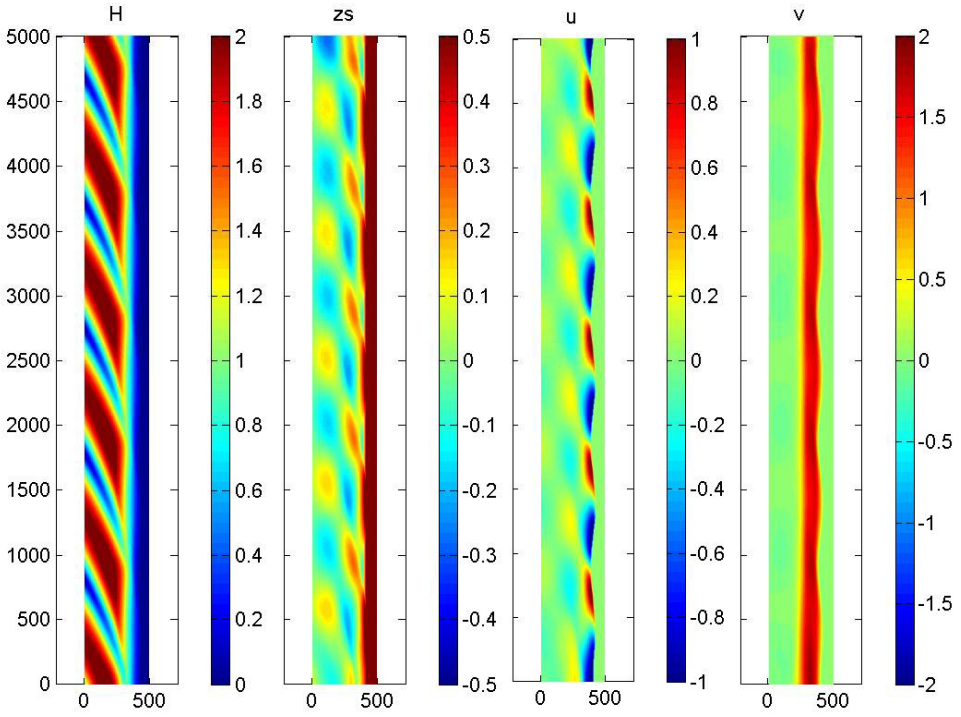

Figure 3 Schematic test of development of edge waves and longshore current. From left to right: short wave height, LF water level, LF cross-shore velocity, LF longshore velocity (snapshot)

Extreme inundation
The Xbeach model was applied to the case over overwash over a dune due to a rising tide. A 2D domain was constructed with a synthetic dune and two bodies of water ("sea" and "bay") on either side. The initial water level at the sea side was 0.8 m and at the bay side - 2 m. The dune has a crest elevation of + 2 meters with a gap which depressed the crest height locally by 1 meter and rests on an otherwise flat bottom at - 4 m. The domain spans 600 meter across and 400 meters along the dune with grid sizes of 4 meters crossdune and 10 meter along the dune.

The water level at the sea side was forced to rise monotonically to +1.5 meters. When the level reaches +1 meter, the dune starts to overflow, and causes erosion in the gap. Figure x shows the progression of the morphodynamic change (black solid line) at the center line of the domain under the water level (blue solid line), while the initial bathymetry is the blackdotted line. The model results show the development of an overwash fan at the bay side

of the dune, but also the development of anti-dunes which are caused by the supercritical flow through the gap. The red line in the figure is the Froude number which fluctuates but in the early stages of the overwash process is well above one. The anti-dunes migrate upstream and cause undulations in the flow, which shows intermittent patterns of super and subcritical flow (hydraulic jumps). At the end of the simulation the dune is severely eroded, at place below the original flat bottom level.

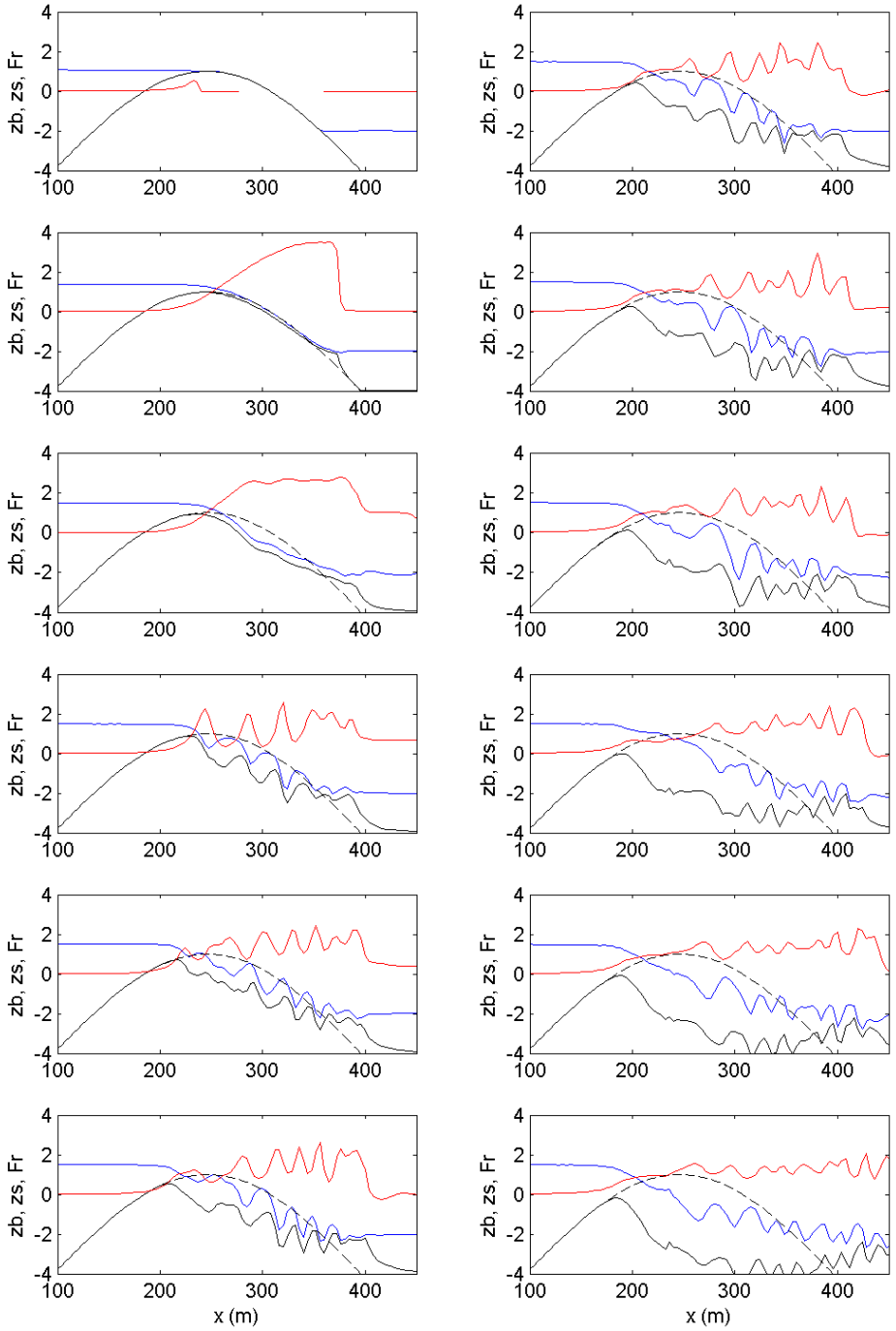

Figure 4 Development of center cross-section of extreme inundation test. Black dashed: initial profile; black: actual bottom profile; blue: actual water level; red: Froude number.

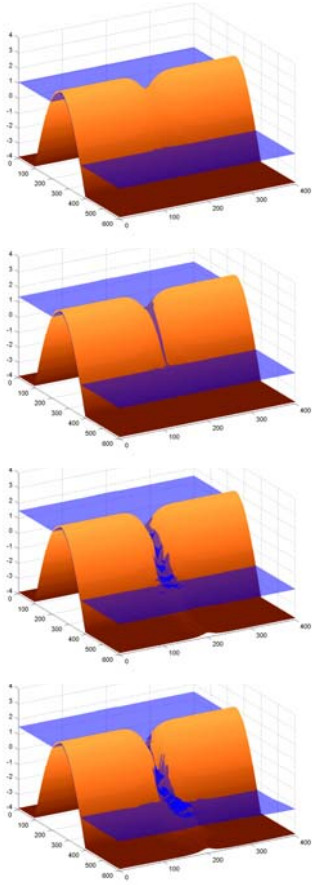

Figure 5 shows 2D images of the dune overwash process at some of the stages of the process at Figure 4.

Although these results are very preliminary and much needs to be checked, the behaviour of the model appears to be physically correct and robust.

Figure 5 3D images of different stages of the breaching process.

7 CONCLUSIONS AND NEXT STEPS

A robust and physics-based public-domain model has been developed with which the various stages in hurricane impacts on barrier coasts can be modeled seamlessly. The potential of the model has been shown in a number of analytical, lab and field cases. It is freely available, at the moment through any of the authors, beta testing by others is taking place and we encourage anyone to have a go. The model is set up in a way that it is relatively easy to parallelize and to incorporate it within the MORPHOS framework; both actions are under construction.

ACKNOWLEDGEMENT

The Research reported in this document has been made possible through the support and sponsorship of the U.S. Government through its European Research Office of the U.S. Army., under Contract no. N62558-06-C-2006.

REFERENCES

Arcilla, A. S., J. A. Roelvink, B. A. O'Connor, A. Reniers, and J. A.Jimenez (1994), The Delta flume '93 experiment, in Coastal Dynamics '94, edited by A. S. Arcilla, N. C. Kraus, and S. J. F. Marcel, pp. 488–502, Am. Soc. of Civ. Eng., Reston, Va.

Erikson, L., M. Larson, H. Hanson, 2005. Prediction of swash motion and run-up including the effects of swash interaction. Coastal Engineering 52 (2005) 285–302.

Galappatti, R. (1983), A depth integrated model for suspended transport, Delft Univ. Rep. 83-7, Dep. of Civ. Eng., Delft Univ. of Technol., Delft, Netherlands.

Larson, M., L. Erikson, H. Hanson, 2004. An analytical model to predict dune erosion due to wave impact. Coastal Engineering 51 (2004) 675– 696.

Nairn, R. B., J. A. Roelvink, and H. N. Southgate (1990), Transition zone width and implications for modelling surfzone hydrodynamics, in Coastal Engineering Conference, 1990: Proceedings of the International Conference, edited by B. L. Edge, pp. 68 – 81, Am. Soc. Of Civ. Eng., Reston, Va.

Nishi, R., Kraus, N.C., 1996. Mechanism and calculation of sand dune erosion by storms. Proceedings of the 25th Coastal Engineering Conference, ASCE, pp. 3034– 3047.

Overton, M.F., Fisher, J.S., 1988. Laboratory investigation of dune erosion. Journal of Waterway, Port, Coastal, and Ocean Engineering 114 (3), 367– 373.

Phillips, O. M. (1977), The Dynamics of the Upper Ocean, 2nd ed., 336 pp., Cambridge Univ. Press, New York.

Raubenheimer, B. and R.T. Guza, 1996. Observations and predictions of run-up. J. of Geophys. Res., vol. 101, no. C10, pp. 25,575-25,587, Nov. 15, 1996.

Reniers, A.J.H.M., J.A. Roelvink and E.B. Thornton. 2004a. Morphodynamic modelling of an embayed beach under wave group forcing. J. of Geophysical Res. , VOL. 109, C01030, doi:10.1029/2002JC001586, 2004.

Reniers, A.J.H.M., E. B. Thornton, T. Stanton and J.A. Roelvink, 2004b. Vertical flow structure during Sandy Duck: Observations and Modeling. Coastal Engineering, Volume 51, Issue 3, May 2004, Pages 237-260.

Roelvink, J. A. (1993a), Dissipation in random wave groups incident on a beach, Coastal Eng., 19, 127– 150.

Roelvink, J. A. (1993b), Surf beat and its effect on cross-shore profiles, Ph.D. thesis, 150 pp., Delft Univ. of Technol., Delft, Netherlands.

Roelvink, J.A., T. van Kessel, S. Alfageme and R. Canizares, 2003. Modelling of barrier island response to storms. In: Proc. Coastal Sediments '03, Clearwater, Florida.

Ruessink, B.G., Miles, J.R., Feddersen, F., Guza, R.T. and Elgar, S., 2001. Modeling the alongshore current on barred beaches. J. Geophys. Res. 106, pp. 22451–22463.

Sallenger, A., 2000. Storm impact scale for barrier islands. J. of Coastal Research, Vol. 16, Nr. 3, pp. 890-895.

Schaeffer, H. A. (1994), Edge waves forced by short-wave groups, J. Fluid Mech., 259, 125–148.

Soulsby, R. L. (1997), Dynamics of Marine Sands, Thomas Telford, London.

Soulsby, R. L., L. Hamm, G. Klopman, D. Myrhaug, R. R. Simons, and G. P. Thomas (1993), Wave-current interaction within and outside the bottom boundary layer, Coastal Eng., 21, 41–69.

Steetzel, H.J., 1993. Cross-shore transport during storm surges. PhD thesis Technical University Delft. ISBN 90-9006345-5, CASPARIE publishers, Zwolle.

Stelling, G.S., Duinmeijer, S.P.A. A staggered conservative scheme for every Froude number in rapidly varied shallow water flows. International Journal for Numerical Methods in Fluids. 2003; 43:1329-1354.

Stockdon, H.F., R.A. Holman, P.A. Howd, A.H. Sallenger. Empirical parameterization of setup, swash, and runup. Coastal Engineering 53 (2006) 573–588.

Stive, M. J. F., and H. J. de Vriend (1994), Shear stresses and mean flow in shoaling and breaking waves, in Proceedings of the Twenty-Fourth International Conference, edited by B. L. Edge, pp. 594–608, Am. Soc. Of Civ. Eng., Reston, Va.

Van Dongeren, A., A. Reniers, J. Battjes, and I. Svendsen (2003), Numerical modeling of infragravity wave response during DELILAH, J. Geophys. Res., 108(C9), 3288, doi:10.1029/2002JC001332.

Van Dongeren, A.R. and I.A. Svendsen (1997). An Absorbing-Generating Boundary condition for Shallow Water Models. J. of Waterways, Ports, Coastal and Ocean Engineering, vol. 123, no. 6, pp. 303-313.

Visser, P.J. 1998. Breach growth in sand dikes. Ph.D.-thesis Delft University of Technology, the Netherlands.

Walstra, D.J. and Roelvink, J.A., and Groeneweg, J., 2000. 3D calculation of wave-driven cross-shore currents. Proceedings 27th International Conference on Coastal Engineering, July 16-21, 2000, Sydney